

# Real-world Instance-specific Image Goal Navigation: Bridging Domain Gaps via Contrastive Learning

1<sup>st</sup> Taichi Sakaguchi  
Graduate School of Info. Sci. & Eng.  
Ritsumeikan University, Osaka, Japan  
sakaguchi.taichi@em.ci.ritsumei.ac.jp

2<sup>nd</sup> Akira Taniguchi\*  
College of Info. Sci. & Eng.  
Ritsumeikan University, Osaka, Japan  
a.taniguchi@em.ci.ritsumei.ac.jp

3<sup>rd</sup> Yoshinobu Hagiwara<sup>†</sup>  
Faculty of Sci. and Eng.  
Soka University, Tokyo, Japan  
hagiwara@soka-u.jp

4<sup>th</sup> Lotfi El Hafi  
Research Organization of Sci. & Tech.  
Ritsumeikan University, Shiga, Japan  
lotfi.elhafi@em.ci.ritsumei.ac.jp

5<sup>th</sup> Shoichi Hasegawa  
Graduate School of Info. Sci. & Eng.  
Ritsumeikan University, Osaka, Japan  
hasegawa.shoichi@em.ci.ritsumei.ac.jp

6<sup>th</sup> Tadahiro Taniguchi<sup>†</sup>  
Graduate School of Informatics  
Kyoto University, Kyoto, Japan  
taniguchi@i.kyoto-u.ac.jp

**Abstract**—Improving instance-specific image goal navigation (InstanceImageNav), which involves locating an object in the real world that is identical to a query image, is essential for enabling robots to help users find desired objects. The challenge lies in the domain gap between the low-quality images observed by the moving robot, characterized by motion blur and low resolution, and the high-quality query images provided by the user. These domain gaps can significantly reduce the task success rate, yet previous work has not adequately addressed them. To tackle this issue, we propose a novel method: few-shot cross-quality instance-aware adaptation (CrossIA). This approach employs contrastive learning with an instance classifier to align features between a large set of low-quality images and a small set of high-quality images. We fine-tuned the SimSiam model, pre-trained on ImageNet, using CrossIA with instance labels based on a 3D semantic map. Additionally, our system integrates object image collection with a pre-trained deblurring model to enhance the quality of the observed images. Evaluated on an InstanceImageNav task with 20 different instance types, our method improved the task success rate by up to three-fold compared to a baseline based on SuperGlue. These findings highlight the potential of contrastive learning and image enhancement techniques in improving object localization in robotic applications. The project website is <https://emergentsystemlabstudent.github.io/DomainBridgingNav/>.

**Index Terms**—contrastive learning, few-shot domain adaptation, instance-specific image goal navigation, 3D semantic map

## I. INTRODUCTION

The importance of solving **instance-specific image goal navigation (InstanceImageNav)** [1] for robots to effectively search for specific instances in complex real-world domestic environments. In this task, the robot locates an object in a query image provided by the user, as shown in Fig. 1 (top). This task becomes even more difficult when multiple instances

This work was supported by JSPS KAKENHI Grants-in-Aid for Scientific Research (Grant Numbers JP23K16975, 22K12212) and JST Moonshot Research & Development Program (Grant Number JPMJMS2011).

\*Corresponding author.

<sup>†</sup> They are also affiliated with the Research Organization of Sci. & Tech., Ritsumeikan University, Shiga, Japan.

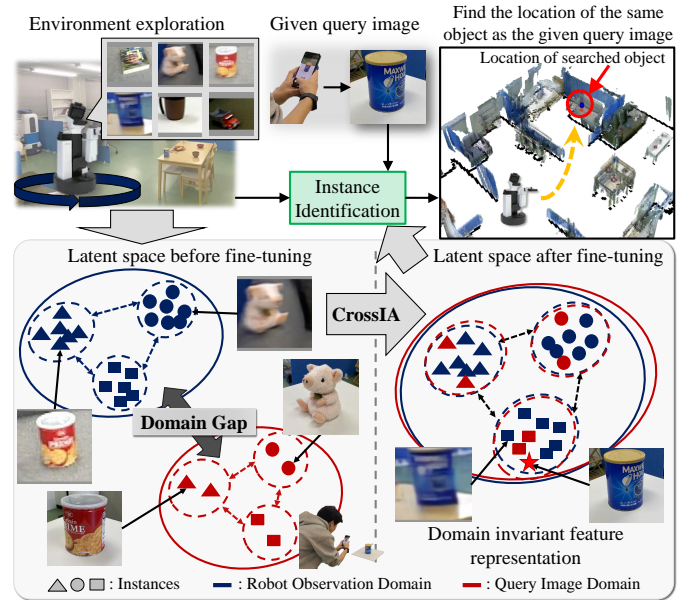


Fig. 1. Focused task in this study. (Top) The robot identifies the position of an object shown in a query image provided by a user's mobile phone. (Bottom left) Domain gap that the image quality significantly differs between the image taken by the user's mobile phone and the object image observed by the real robot. (Bottom right) Contrastive learning to align images of the same instance with different image quality in latent space.

of the same object class, each with a distinct appearance, are present in the environment. To successfully execute tasks in such scenarios, robots must be able to distinguish between different instances of the same class of objects. If the target instance can be visually differentiated from others, the robot can successfully locate an object identical to the provided query image.

The challenge in real-world environments is the **domain gap** between the low-quality images captured by the robot and the high-quality images provided by users (see Fig. 1 (bottom left)). This discrepancy in image quality significantly reduces the success rate of InstanceImageNav. When robots explore

an environment, the images they capture are often low-quality due to motion blur, low resolution from movement, and the limitations of their onboard sensors. Objects may appear small in the robot’s field of view (see Fig. 2 (top)), further reducing image quality. This issue is particularly pronounced in data collected by consumer robots used in a domestic setting, where the field angle of view and image quality may be insufficient. Hence, it is important to bridge the domain gap between the robot’s observed images and the query images provided by the user (see Fig. 1 (bottom right)). Additionally, while the robot can collect many images, the user can only provide a limited number of environment-specific images without significant effort.

To address this challenge, we propose a system that integrates two key mechanisms: one for **learning invariant feature representations between massive low-quality and a few high-quality images** and another for enhancing the quality of images observed by robots using a pre-trained deblurring model [2]. This system is based on an object image database construction system [3]. For the first mechanism, we propose a **few-shot cross-quality instance-aware adaptation (CrossIA)** through contrastive learning with an instance classifier. Contrastive learning enables the acquisition of invariant feature representations between images of the same instance in different domains [4], [5]. The 3D semantic map constructed through environment exploration automatically provides instance labels to the database. We evaluated the performance in identifying the object identical to the query image from the object images collected by the robot while exploring the real-world environment. The located objects are 20 different instances that can be placed on a table. Our main contributions are two-fold.

- 1) We show that combining contrastive learning with few-shot learning and an instance classifier is essential for learning invariant feature representations between cross-quality images under few-shot conditions, effectively bridging the domain gap that cannot be resolved by deblurring alone.
- 2) We experimentally demonstrate that the proposed method improves task success rates by up to three-times better than existing methods, SuperGlue [6], highlighting its potential to identify small everyday objects in real-world InstanceImageNav.

The remainder of this paper is organized as follows. Section II presents the problem statement, detailing the specific challenges addressed by our study. Section III provides an overview of the related work. Section IV describes the proposed method. Section V describes our experimental protocols and metrics. Section VI presents and discusses our results. Finally, Section VII concludes with directions for future work.

## II. PROBLEM STATEMENT

This study addressed the essential challenges for the advancement of InstanceImageNav in the real world.

**Domain gap by image quality disparity:** The domain gap between the low-quality images captured by robots and

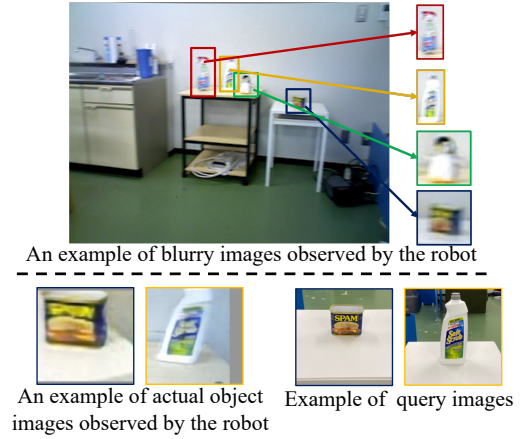


Fig. 2. (Top) Object images cropped from the robot’s observation image; (Bottom left) Examples of low-quality images; (Bottom right) Examples of high-quality images as the query.

the high-quality query images provided by users is a major challenge. This gap stems from motion blur, low resolution, and other factors that diminish image quality when robots are in motion. Consequently, the robot’s capability to match these images with high-quality query images is greatly hindered.

**Limited robustness of previous work:** Most current InstanceImageNav approaches have been developed and tested in the Habitat Simulator [7], which does not account for real-world challenges such as motion blur [1], [8], [9]. Furthermore, previous work on InstanceImageNav [1], [3], [8] often targets large and easily distinguishable objects, such as `chair`, `desk`, and `television`. However, robots might need to locate smaller or visually similar objects that are more common in practical scenarios, such as `cups`, `bottles`, and `books`. When collecting images of such objects, the resolution tends to be low and image quality may differ from the query image provided by the user (see Fig. 2 (bottom)).

## III. RELATED WORK

### A. Object Searching

The search for objects is classified into three types based on the representation of the search target. First, object goal navigation (ObjectNav) involves locating any object belonging to a given class, such as `book` [10]. Second, vision-and-language navigation (VLN) involves locating an object represented by language instructions such as “Go to the living room and pick up the yellow cup on the square table” [11], [12]. This method also enables the search for specific instances [12]. However, these language instructions require the user to know where the target object is located within the environment. When the user is unaware of the object’s location, the ability to locate an object identical to a query image captured by the user becomes crucial. Therefore, addressing InstanceImageNav is essential for developing the capability to search for specific instances.

Methods for object searching can be broadly categorized into two types. One type is the end-to-end method, which involves learning neural networks that directly generate actions

from the robot’s observed images using deep reinforcement learning or imitation learning [1], [10], [13]. The other type is the modular method, which integrates components such as pre-trained object recognition and simultaneous localization and mapping (SLAM) [3], [8]–[10]. The end-to-end method suffers from sample inefficiency [1] and poor sim-to-real transfer [14]. Therefore, we also propose a modular navigation system.

To solve InstanceImageNav, previous work proposed navigation systems that combine multiple techniques [3], [8], [9]. For instance, Chang *et al.* proposed a system exploring the environment and constructing a database that saves 3D semantic maps and images of each instance [3]. They execute InstanceImageNav using the local feature matching, Super-Glue [6], to search for the same object as the given query image from the database and identify its position on the 3D semantic map.

### B. Contrastive Learning

Contrastive learning is a form of self-supervised learning that involves learning from tasks that contrast different images of the same instance [15]–[18]. Models pre-trained with contrastive learning are known for acquiring discriminative feature representations that effectively differentiate instances within the same class [19]. For instance, Ido *et al.* demonstrated high precision in image classification tasks at both the instance and class levels using features extracted from an image encoder trained with contrastive learning, combined with the k-nearest neighbor method [19]. Consequently, models trained via contrastive learning are deemed well-suited for the InstanceImageNav task.

SimView improved performance on InstanceImageNav by fine-tuning a pre-trained SimSiam [17] with contrastive learning using instance labels derived from a 3D semantic map [9]. This approach forms the basis for this study. However, it has not yet been tested for domain gaps on real robots.

### C. Domain-Invariant Feature Learning

In the InstanceImageNav, the images of objects observed by the robot are low-quality, while the provided query images are high-quality. Thus, learning instance-wise domain-invariant feature representations between high-quality and low-quality images could improve the success rate of the task.

Adversarial learning has been utilized to learn domain-invariant feature representations [20], [21]. This approach enables networks to learn domain-invariant feature representations by back-propagating the reverse gradients of the domain classifier. However, this approach might overlook discrimination between instances.

However, methods using contrastive learning to obtain domain-invariant feature representations have been proposed [4], [5]. Since contrastive learning enables networks to learn instance discriminative representations [19], approaches based on contrastive learning could learn instance-wise domain-invariant feature representations. Therefore, this study focuses on contrastive learning. A significant difference from previous work [4], [5] is that only a few samples are available in this study for one domain.

### D. Motion Deblurring

Motion blur occurs when the camera or the subject moves during the sensor’s exposure time. Therefore, images obtained from the sensors of a moving robot are likely to be blurred. Motion blur degrades the recognition accuracy of pre-trained image recognition models [22]. Therefore, navigation systems that search for objects while in motion require mechanisms to remove image blur.

Deblurring methods can be broadly categorized into two types. One is formulating the deblurring as an optimization problem [23]–[25]. This approach involves optimizing the blur kernel from the blurred image to the sharp image using gradient descent. The other is a learning-based approach. In this approach, neural networks are trained to restore sharp images from blurred images using pairs of blurred and sharp images [2], [22]. Formulating deblurring as an optimization problem has a high computational cost. Therefore, we utilize a learning-based deblurring method [2].

## IV. PROPOSED SYSTEM

As shown in Fig. 3, the proposed system is divided into three main modules. First, the data collection module constructs the 3D semantic map of the environment and then collects object images. Second, the fine-tuning module fine-tunes the pre-trained models using the collected object images and few-shot high-quality images provided by a user through contrastive learning. Our contrastive learning is called a few-shot cross-quality instance-aware adaptation (CrossIA). Finally, the navigation module leverages the fine-tuned model and the semantic map to locate objects identical to the query image.

### A. Data Collection Module

The data collection module constructs a 3D semantic map from sequence data of RGBD images and camera poses collected by a robot moving in 3D space. The construction of the 3D semantic map involves projecting instance ID information onto a voxel-based 3D map [26]. However, while Kanechika *et al.* construct a 3D semantic map by projecting the class label IDs obtained from the semantic segmentation results, we utilize fast segment anything (FastSAM) [27] to construct the 3D semantic map by projecting instance ID information onto the 3D map. To ensure that the constructed 3D map has consistent label IDs from frame to frame, we employ 3D semantic mapping method [28] similar to Kanechika *et al.*’s approach [26].

First, RGB images collected by the robot exploring the environment are entered into the multiscale stage network [2] for deblurring. Next, FastSAM segments images element by element. The 3D semantic map is then constructed using the segmentation results, depth images, and camera poses.

During this process, 2D segmentation masks are generated from the 3D semantic map using a method called ray tracing. These rays interact with the 3D map, and the instance ID of the first collision detected by the rays is captured. This results in the creation of a mask image that corresponds to the segmented

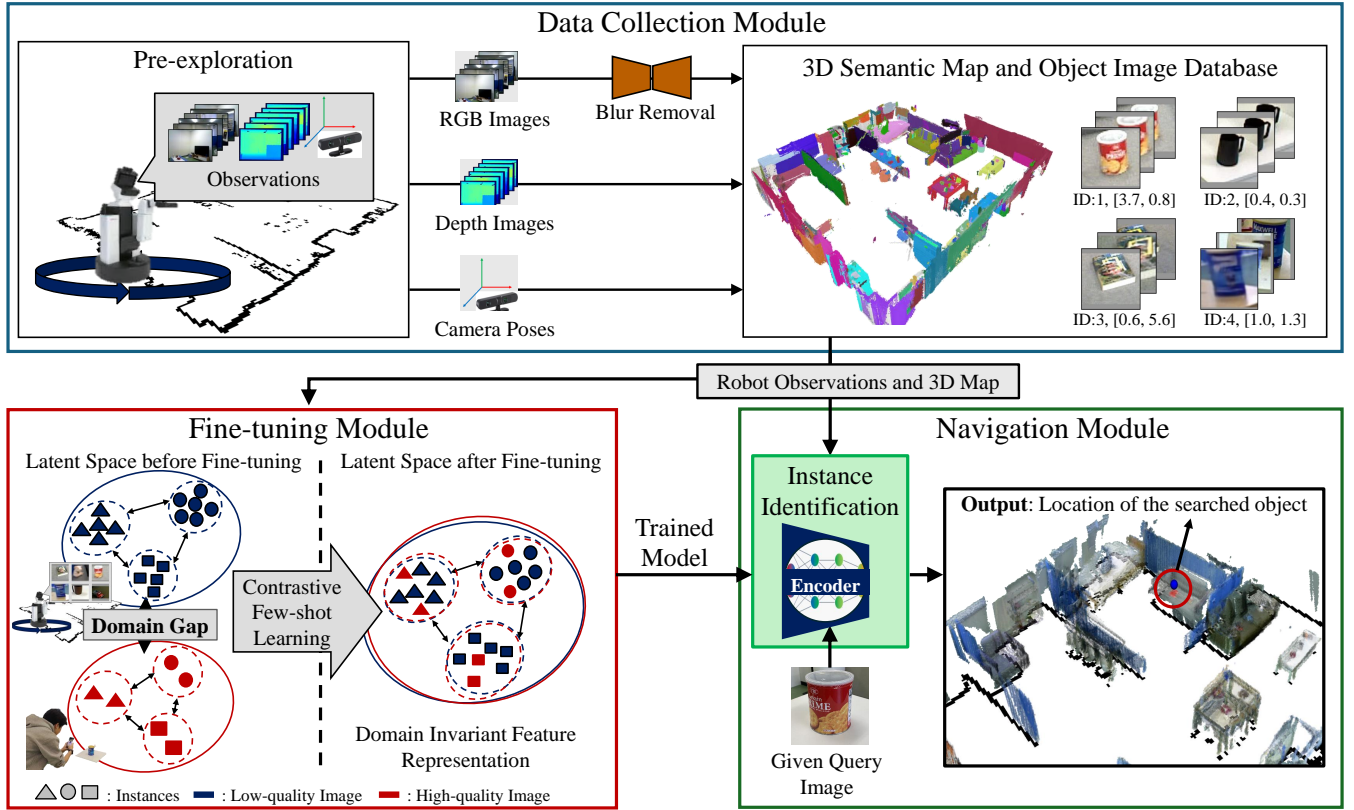


Fig. 3. The overall diagram of the proposed system. The proposed system automatically collects object images from RGBD images and camera pose time series data collected by a robot that explored the environment in advance. The object image database stores images along with their corresponding ID and position coordinates (e.g., "ID:1, [3.7, 0.8]"). The fine-tuning module fine-tunes the pre-trained image encoder using the collected object images. The navigation module identifies the position of the object identical to the given query image using a fine-tuned image encoder.

area of the 3D map. This method ensures that pseudo-labels are consistently generated for images of the same instance across different frames. Once the mask images are created, they are transformed into bounding boxes (BBoxes). These bounding boxes are used to extract specific regions from the RGB images, allowing for the collection of object images that correspond to the segmented areas.

### B. Fine-tuning Module

This module fine-tunes a pre-trained image encoder by the contrastive learning between low-quality images observed by the robot and few-shot high-quality images provided by the user. SimSiam, a negative free contrastive learning method, can learn with a small batch size [17]. In contrast, contrastive learning methods require negative pair learning with a large batch size [15]. Therefore, we utilize SimSiam for fine-tuning.

Additionally, for training, the user must capture a few images of the objects they want the robot to locate using a mobile device and provide these images to the robot. The process is relatively simple and involves only a small number of images, so the user is not significantly burdened.

Fine-tuning the image encoder involves contrastive learning between high-quality and low-quality images, and the contrastive learning between images the robot observed, as shown in Fig. 4. Furthermore, minimizing the losses associated

with contrastive learning and the linear classifier during fine-tuning of a pre-trained image encoder reduces the variance of feature vectors between images with the same label [9], [29]. Consequently, we perform fine-tuning of the image encoder by adding a linear classifier to SimSiam, as illustrated in Fig. 4. The labels required for calculating the linear classifier's loss are obtained using pseudo-labels automatically generated by the data collection module. Thus, the loss function during fine-tuning can be expressed as follows:

$$\mathcal{L} = \sum_{m=1}^M \mathcal{L}_m^{\text{robot}} + \sum_{n=1}^N \mathcal{L}_n^{\text{cross}}, \quad (1)$$

where  $M$  and  $N$  represent the number of pairs of low-quality images and the number of pairs of high-quality and low-quality images, for the same instance in a mini-batch, respectively. Loss functions  $\mathcal{L}_m^{\text{robot}}$  and  $\mathcal{L}_n^{\text{cross}}$  are calculated as follows:

$$\begin{aligned} \mathcal{L}_m^{\text{robot}} = & -\frac{1}{2} \{ \text{CosSim}(p_m^l, \tilde{z}_m^l) + \text{CosSim}(\tilde{p}_m^l, z_m^l) \} \\ & + \frac{1}{2} \{ \text{CE}(y_m^l, y_m^*) + \text{CE}(\tilde{y}_m^l, y_m^*) \}, \end{aligned} \quad (2)$$

$$\begin{aligned} \mathcal{L}_n^{\text{cross}} = & -\frac{1}{2} \{ \text{CosSim}(p_n^l, z_n^h) + \text{CosSim}(p_n^h, z_n^l) \} \\ & + \frac{1}{2} \{ \text{CE}(y_n^h, y_n^*) + \text{CE}(y_n^l, y_n^*) \}, \end{aligned} \quad (3)$$



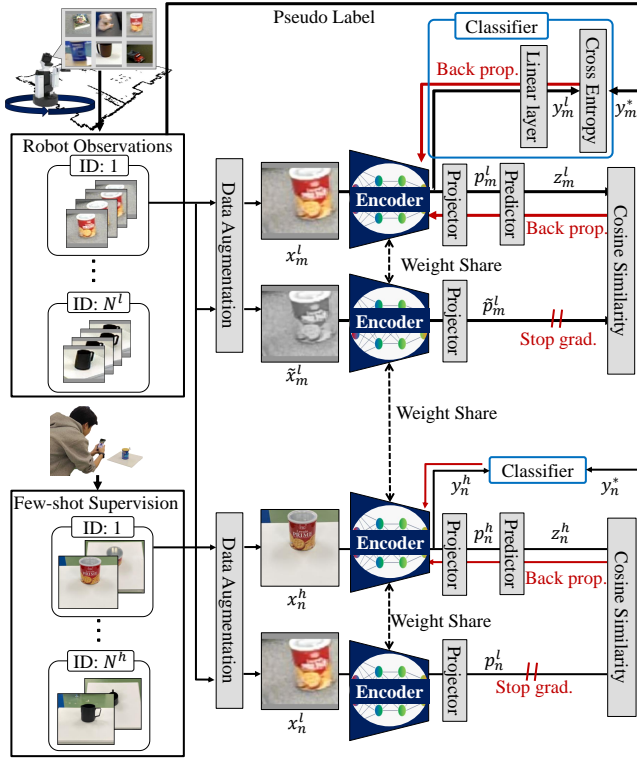


Fig. 4. The fine-tuning by few-shot cross-quality instance-aware adaptation. Two contrasting images are swapped and processed in the same way.

where  $\text{CosSim}()$  and  $\text{CE}()$  denote cosine similarity and cross-entropy. Variables  $p$  and  $z$  with a certain subscript are the outputs of SimSiam’s projector and predictor, respectively. The superscripts  $l$  and  $h$  denote that they are derived from low- and high-quality images. The same applies to the variables with tildes. Here,  $x$  and  $\tilde{x}$  are different images for the same object generated by data augmentation. A variable  $y$  is the prediction ID when the image  $x$  is classified.  $y^*$  is the pseudo-label of the instance obtained from the data collection module.

### C. Navigation Module

As shown in Fig. 3, the navigation module finds the object that matches the given query image. It uses images collected by the data collection module, the 3D semantic map, and feature vectors from the fine-tuned image encoder.

First, the fine-tuned image encoder is utilized to compute the feature vectors  $z_{\text{obs}}$  and  $z_{\text{query}}$  for the object images collected by the data collection module and query image, respectively. Using these feature vectors, the similarity between the query and observed object images is calculated using the cosine similarity shown as follows:

$$\text{CosSim}(z_{\text{query}}, z_{\text{obs}}) = \frac{z_{\text{query}}}{\|z_{\text{query}}\|_2} \cdot \frac{z_{\text{obs}}}{\|z_{\text{obs}}\|_2}. \quad (4)$$

Subsequently, the instance with the highest similarity to the query image is identified.

Next, the module identifies the centroid coordinates of the object on the 3D map that best matches the query image, and the robot moves towards it. The centroid is calculated

by averaging the 3D coordinates of the voxels with the same ID as the identified object. However, navigation can fail if the centroid’s location overlaps with an occupied position on the map. To address this, the module selects an unoccupied area within a 1.0 m radius from the object’s centroid as the navigation target. This distance is based on Krantz *et al.*’s definition of the success criteria for the InstanceImageNav task, where the distance between the target object and the robot is defined as 1.0 m or less [1].

## V. EXPERIMENTS

If our proposed system can accurately identify the object that matches the query image within the observed images using the navigation module, then moving to the target object should be feasible. Therefore, in this experiment, we evaluate the system by checking how well it identifies the object that matches the query image from the observed images. This experiment has two main objectives:

- 1) To determine if introducing deblurring during exploration in the environment can improve the success rates.
- 2) To assess whether fine-tuning a pre-trained model using contrastive learning with both images observed by the robot and a few high-quality images provided by the user can enhance success rates.

In addition, to evaluate the impact of using a few high-quality images during fine-tuning, we examined how task success rates improve and how they decline as fewer images are provided for each object.

The system was developed using a software development environment [30].

### A. Comparison Methods

We compare SuperGlue [6], SimSiam [17], SimView [9], and the proposed CrossIA. SuperGlue was utilized in previous work on InstanceImageNav [3], [8]. SimSiam used a pre-trained model on open dataset [31], [32]. SimView is equivalent to the case where only Eq. (2) is employed and also serves as an ablation study for the proposed method. In addition, we evaluated a method to learn domain-invariant feature representations by combining contrastive learning and adversarial learning with domain labels [20]. Domain-invariant feature representation can be learned even when the amount of high-quality images provided during training is small.

### B. Conditions and Dataset

The robot observation data collected in this experiment were obtained using the Human Support Robot (HSR) [33] built by Toyota Motor Corporation. Additionally, the RGBD sensor attached to the HSR is the Asus Xtion Pro Live. This camera can capture RGB images with a resolution of  $640 \times 480$  at 30 fps. The RGBD sensor is mounted about 1 m above the ground. During data collection, the robot moved throughout the environment without stopping in front of specific objects, and the entire  $74 \text{ m}^2$  area was scanned in 2 min to construct a 3D semantic map [28]. This exploration collected 606 RGBD

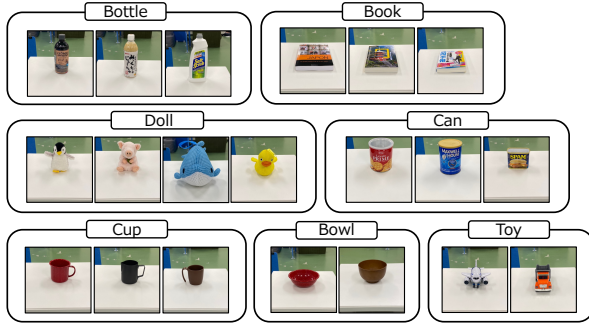


Fig. 5. Instances targeted for search in this experiment.

images. The constructed dataset contains 145 instances, and 2011 images were collected by the robot.

The high-quality images for each instance were captured using the camera on an iPhone 11 Pro. We provided five high-quality images for each instance for fine-tuning. They are all different arrangements and backgrounds in the environment. Additionally, we conducted ablation studies comparing one, three, and five images.

The robot locates 20 instances from the classes `Bottle`, `Book`, `Cup`, `Can`, `Bowl`, `Doll`, and `Toy`, as shown in Fig. 5. The query images were taken from distances of 40 cm. When capturing the images, the photographer took pictures from eight different angles, both standing and crouching, resulting in 32 images for each instance. Note that the high-quality images used for training and testing are different.

### C. Training Set-up

The PCs are equipped with an Intel Core i9-9900K CPU, 64GB RAM, and an Nvidia RTX 2080 GPU for training, excluding SimView, and an Intel Core i9-14900KF CPU, 64GB RAM, and an Nvidia RTX 4090 GPU for training with SimView and all evaluation. The optimizer used for all conditions was stochastic gradient descent. The batch size was set to 256 and the learning rate was 0.07. The training was conducted for 1000 epochs. These hyperparameters were chosen to ensure consistency and comparability in our experiments. Four types of data augmentation were used during the training: crop and resize, color jitters, grayscale, and horizontal flip.

### D. Evaluation Metrics

The evaluation metrics for the task include the success rate (SR), the mean reciprocal rank (MRR) [34], and the mean rank (MR). SR evaluates how accurately the object matching the query image is identified as the most similar object among the images observed by the robot. MRR measures how well the object matching the query image is identified at higher ranks. Thus, they can be expressed as follows:

$$\text{SR} = \frac{1}{N} \sum_{n=1}^N s_n, \quad \text{MRR} = \frac{1}{N} \sum_{n=1}^N \frac{1}{k_n}, \quad (5)$$

where  $N$  is the number of trials and  $N = 640$  (i.e. 20 instances  $\times$  32 images). for this study. In Eqs. (5),  $s_n$  represents a binary

TABLE I  
SCORE RESULTS OF COMPARISON METHODS

Methods	Deblurring	SR $\uparrow$	MRR $\uparrow$	MR $\downarrow$
SuperGlue [6]	—	0.275	0.365	2.73
SuperGlue [6]	✓	0.281	0.370	2.70
SimSiam [17]	—	0.293	0.413	2.41
SimSiam [17]	✓	0.290	0.416	2.40
SimView [9]	—	0.066	0.115	8.64
SimView [9]	✓	0.034	0.097	10.3
CrossIA (Ours)	✓	<b>0.751</b>	<b>0.812</b>	<b>1.24</b>
CrossIA with [20]	✓	<u>0.753</u>	<u>0.820</u>	<u>1.21</u>

TABLE II  
SCORES OF FINE-TUNED SIMSIAM BASED ON FEW-SHOT CONDITIONS

Methods	SR $\uparrow$	MRR $\uparrow$	MR $\downarrow$
One-shot	0.421 (0.587)	0.548 (0.696)	1.82 (1.43)
Three-shot	0.646 (0.690)	0.752 (0.763)	1.32 (1.31)
Five-shot	0.751 (0.753)	0.812 (0.820)	1.24 (1.21)

The numbers in parentheses are the results with the addition of adversarial learning [20].

variable indicating whether the task was successful for each instance, where  $s_n = 1$  if the query image task was successful and  $s_n = 0$  otherwise.  $k_n$  is the rank at which the same object as the query image is retrieved.

MR is the reciprocal of MRR and indicates the average rank at which the object matching the query image was found across all trials of the task.

## VI. RESULTS

### A. Effectiveness of CrossIA on Baselines

Table I shows the metric scores under the conditions listed. Firstly, comparing the evaluation metrics of the baselines SuperGlue and the proposed method, we observe a 2.7-fold improvement in SR and a 2.2-fold improvement in MRR with the proposed method. While SuperGlue typically ranks the matching object third on average across all trials, the proposed method consistently ranks it first. Additionally, when comparing metrics between the pre-trained SimSiam and the proposed method, the SR score improves by 2.6-fold and the MRR score improves by 2.0-fold with the proposed method. In contrast, SimView showed a much lower success rate due to fine-tuning with only low-quality observation images from the robot. Furthermore, incorporating adversarial learning into the proposed method did not result in a significant improvement over the version without adversarial learning.

### B. Effect of Deblurring on Task Success Rate

When comparing metric scores with and without deblurring in pre-trained models, no significant difference is observed under any conditions. This suggests that learning domain-invariant feature representations is more effective in improving the task success rate than simply removing blur from the robot’s observed images.

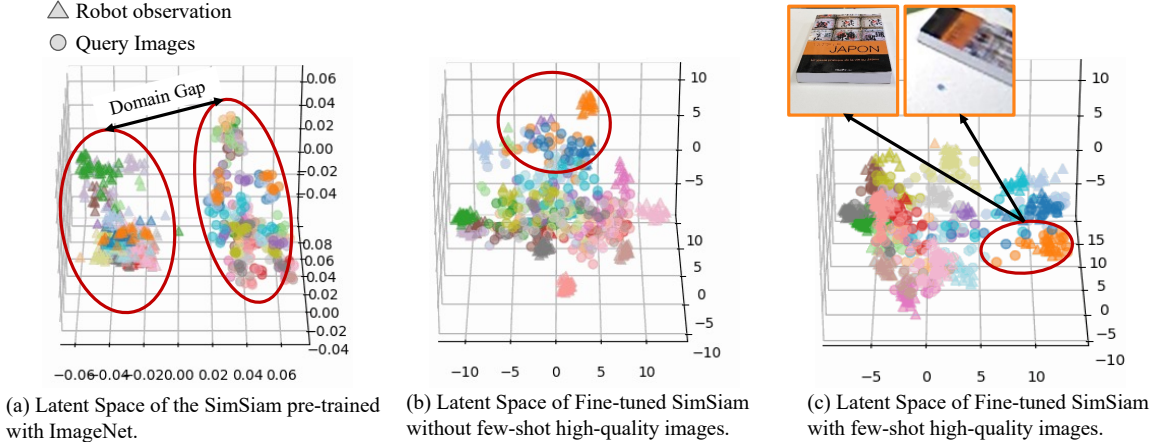


Fig. 6. Latent spaces of the image encoders for different training conditions. (a) SimSiam: Data between different domains are spatially separated. (b) SimView: Only low-quality images of the same instance are closer together, as shown in the region marked by the red ellipse. (c) CrossIA: Images from different domains of the same instance move closer in the latent space.

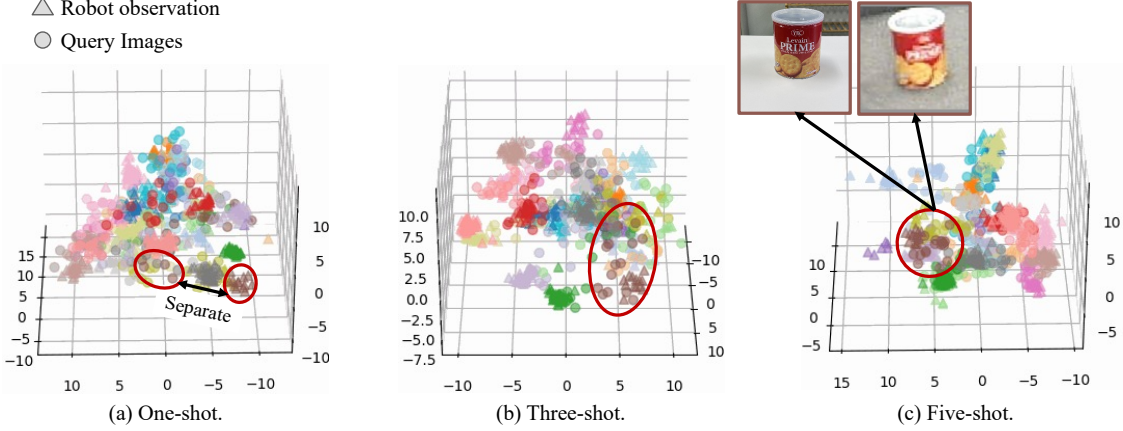


Fig. 7. Comparison of latent spaces acquired under different training conditions, including those where the model was trained with robot observations and a few high-quality images, reveals the following: As indicated by the red ellipse in each figure, providing more high-quality images during training leads to a closer alignment of images from different domains in the latent space.

### C. Qualitative Analysis of Latent Space

We compare the distribution of query images (○) and robot observation images (△) in the latent spaces using both pre-trained and fine-tuned SimSiam methods, as shown in Fig. 6. In the latent space of the pre-trained SimSiam (Fig. 6(a)), high-quality and low-quality images are clearly separated. In the latent space of the Simview, which was trained only with robot observation images, the observed images of the same instance are clustered closely together (Fig. 6(b)). However, the high-quality query images remain distinct from these observed images. This suggests that query images of different instances are not well separated in the latent space, likely due to overfitting to the identification of low-quality images. In the latent space of CrossIA (Fig. 6(c)), images of the same instance from different domains are clustered closely together. These results indicate that contrastive learning with images of the same instance across different domains, as employed in the proposed method, enhances the task success rate.

### D. Influence of Few-Shot Learning on Performance

Table II shows the metrics scores for a varying number of high-quality images during learning. The task success rate decreases as the number of high-quality images provided during training decreases. As shown in Fig. 7, images from different domains tend to cluster more closely in the latent space as the number of high-quality images increases. This result suggests that providing a sufficient number of high-quality images during training improves the ability to learn domain-invariant feature representations through contrastive learning.

Under one-shot conditions, adding adversarial learning improved all evaluation metric scores compared to using only contrastive learning, as shown in Table II. This result suggests that combining adversarial and contrastive learning can bring images from different domains closer together in the latent space, even with fewer high-quality images than when using contrastive learning alone.

## VII. CONCLUSION

In this study, we proposed a method to address the reduced success rates in InstanceImageNav due to the domain gap between robot-observed images and user-provided images. Our approach leverages a few high-quality images along with robot observations to bridge this gap. Specifically, we introduced CrossIA, a method that employs contrastive learning to develop domain-invariant feature representations between robot-observed images and high-quality few-shot images. Experimental results demonstrated that the task success rate improved three-fold compared to SuperGlue. Additionally, the impact of deblurring on task success rates was found to be limited.

A limitation of the proposed method is its reliance on users providing a few high-quality images for each object. Although the method is designed to work effectively with a small number of images, the need for high-quality images increases as the number of objects to be searched grows. This can become impractical in real-world scenarios where obtaining such images for many objects is challenging. Future work should focus on developing methods to reduce or eliminate the dependency on user-provided high-quality images.

Future work will explore the use of advanced image restoration methods, such as pre-trained diffusion models [35], to automatically generate high-quality images from low-quality images captured by robots. This approach could improve the success rate of InstanceImageNav, especially in real-world scenarios with limited high-quality images.

## REFERENCES

- [1] J. Krantz, S. Lee, J. Malik *et al.*, “Instance-Specific Image Goal Navigation: Training Embodied Agents to Find Object Instances,” *arXiv preprint arXiv:2211.15876*, 2022.
- [2] K. Kim, S. Lee, and S. Cho, “MSSNet: Multi-Scale-Stage Network for Single Image Deblurring,” in *European Conference on Computer Vision (ECCV)*, 2022, pp. 524–539.
- [3] M. Chang, T. Gervet, M. Khanna *et al.*, “GOAT: Go to Any Thing,” *arXiv preprint arXiv:2311.06430*, 2023.
- [4] R. Wang, Z. Wu, Z. Weng *et al.*, “Cross-domain Contrastive Learning for Unsupervised Domain Adaptation,” *IEEE Transactions on Multimedia*, 2022.
- [5] A. Singh, “CLDA: Contrastive Learning for Semi-Supervised Domain Adaptation,” *Advances in Neural Information Processing Systems (NeurIPS)*, vol. 34, pp. 5089–5101, 2021.
- [6] P.-E. Sarlin, D. DeTone, T. Malisiewicz *et al.*, “SuperGlue: Learning Feature Matching with Graph Neural Networks,” in *IEEE/CVF Computer Vision and Pattern Recognition Conference (CVPR)*, 2020, pp. 4938–4947.
- [7] M. Savva, A. Kadian, O. Maksymets *et al.*, “Habitat: A Platform for Embodied AI Research,” in *IEEE/CVF International Conference on Computer Vision (ICCV)*, 2019, pp. 9339–9347.
- [8] J. Krantz, T. Gervet, K. Yadav *et al.*, “Navigating to Objects Specified by Images,” in *IEEE/CVF International Conference on Computer Vision (ICCV)*, 2023, pp. 10916–10925.
- [9] T. Sakaguchi, A. Taniguchi, Y. Hagiwara *et al.*, “Object instance retrieval in assistive robotics: Leveraging fine-tuned simsiam with multi-view images based on 3d semantic map,” in *IEEE/RSJ International Conference on Intelligent Robots and Systems (IROS)*, 2024.
- [10] B. Li, J. Han, Y. Cheng *et al.*, “Object Goal Navigation in Embodied AI: A Survey,” in *International Conference on Video, Signal and Image Processing (VSIP)*, 2022, pp. 87–92.
- [11] J. Gu, E. Stefani, Q. Wu *et al.*, “Vision-and-Language Navigation: A Survey of Tasks, Methods, and Future Directions,” *Association for Computational Linguistics (ACL)*, pp. 7606–7623, 2022.
- [12] K. Kaneda, S. Nagashima, R. Korekata *et al.*, “Learning-To-Rank Approach for Identifying Everyday Objects Using a Physical-World Search Engine,” *IEEE Robotics and Automation Letters*, 2024.
- [13] K. Yadav, R. Ramrakhya, A. Majumdar *et al.*, “Offline Visual Representation Learning for Embodied Navigation,” in *Workshop on Reinforcing Reinforcement Learning at International Conference on Learning Representations (ICLR)*, 2023.
- [14] T. Gervet, S. Chintala, D. Batra *et al.*, “Navigating to Objects in the Real World,” *Science Robotics*, vol. 8, no. 79, p. ead6991, 2023.
- [15] T. Chen, S. Kornblith, M. Norouzi *et al.*, “A Simple Framework for Contrastive Learning of Visual Representations,” in *International Conference on Machine Learning (ICML)*, 2020, pp. 1597–1607.
- [16] K. He, H. Fan, Y. Wu *et al.*, “Momentum Contrast for Unsupervised Visual Representation Learning,” in *IEEE/CVF Computer Vision and Pattern Recognition Conference (CVPR)*, 2020, pp. 9729–9738.
- [17] X. Chen and K. He, “Exploring Simple siamese Representation Learning,” in *IEEE/CVF Computer Vision and Pattern Recognition Conference (CVPR)*, 2021, pp. 15 750–15 758.
- [18] J.-B. Grill, F. Strub, F. Altché *et al.*, “Bootstrap Your Own Latent: A New Approach to Self-Supervised Learning,” in *Advances in Neural Information Processing Systems (NeurIPS)*, vol. 33, 2020, pp. 21 271–21 284.
- [19] I. Ben-Shaul, R. Shwartz-Ziv, T. Galanti *et al.*, “Reverse Engineering Self-Supervised Learning,” *Advances in Neural Information Processing Systems (NeurIPS)*, vol. 37, 2023.
- [20] Y. Ganin, E. Ustinova, H. Ajakan *et al.*, “Domain-Adversarial Training of Neural Networks,” *Journal of machine learning research*, vol. 17, no. 59, pp. 1–35, 2016.
- [21] E. Tzeng, J. Hoffman, K. Saenko *et al.*, “Adversarial discriminative domain adaptation,” in *IEEE/CVF Computer Vision and Pattern Recognition Conference (CVPR)*, 2017, pp. 7167–7176.
- [22] O. Kupyn, V. Budzan, M. Mykhailych *et al.*, “DeblurGAN: Blind Motion Deblurring Using Conditional Adversarial Networks,” in *IEEE/CVF Computer Vision and Pattern Recognition Conference (CVPR)*, 2018, pp. 8183–8192.
- [23] S. Cho and S. Lee, “Fast Motion Deblurring,” in *ACM Transactions on Graphics (SIGGRAPH Asia)*, 2009, pp. 1–8.
- [24] Q. Shan, J. Jia, and A. Agarwala, “High-Quality Motion Deblurring from a Single Image,” *ACM Transactions on Graphics (SIGGRAPH)*, vol. 27, no. 3, pp. 1–10, 2008.
- [25] D. Ren, K. Zhang, Q. Wang *et al.*, “Neural Blind Deconvolution using Deep Priors,” in *IEEE/CVF Computer Vision and Pattern Recognition Conference (CVPR)*, 2020, pp. 3341–3350.
- [26] A. Kanachika, L. El Hafi, A. Taniguchi *et al.*, “Interactive Learning System for 3D Semantic Segmentation with Autonomous Mobile Robots,” in *IEEE/SICE International Symposium on System Integration (SII)*, 2024, pp. 1274–1281.
- [27] X. Zhao, W. Ding, Y. An *et al.*, “Fast Segment Anything,” *arXiv preprint arXiv:2306.12156*, 2023.
- [28] K. Tateno, F. Tombari, and N. Navab, “Real-time and Scalable Incremental Segmentation on Dense SLAM,” in *IEEE/RSJ International Conference on Intelligent Robots and Systems (IROS)*, 2015, pp. 4465–4472.
- [29] Y. Zhang, B. Hooi, D. Hu *et al.*, “Unleashing the Power of Contrastive Self-Supervised Visual Models via Contrast-Regularized Fine-Tuning,” *Advances in Neural Information Processing Systems (NeurIPS)*, vol. 34, pp. 29 848–29 860, 2021.
- [30] L. El Hafi, G. A. Garcia Ricardez, F. von Drigalski *et al.*, “Software Development Environment for Collaborative Research Workflow in Robotic System Integration,” *Advanced Robotics*, vol. 36, no. 11, pp. 533–547, 2022.
- [31] A. Dai, A. X. Chang, M. Savva *et al.*, “ScanNet: Richly-annotated 3D Reconstructions of Indoor Scenes,” in *IEEE/CVF Computer Vision and Pattern Recognition Conference (CVPR)*, 2017, pp. 5828–5839.
- [32] J. Deng, W. Dong, R. Socher *et al.*, “ImageNet: A Large-Scale Hierarchical Image Database,” in *IEEE/CVF Computer Vision and Pattern Recognition Conference (CVPR)*, 2009, pp. 248–255.
- [33] T. Yamamoto, K. Terada, A. Ochiai *et al.*, “Development of Human Support Robot as the Research Platform of a Domestic Mobile Manipulator,” *ROBOMECH Journal*, vol. 6, 2019.
- [34] T.-Y. Liu, “Learning to Rank for Information Retrieval,” *Foundations and Trends in Information Retrieval*, vol. 3, no. 3, pp. 225–331, 2009.
- [35] X. Lin, J. He, Z. Chen *et al.*, “Diffbir: Towards blind image restoration with generative diffusion prior,” *arXiv preprint arXiv:2308.15070*, 2023.